AIAA 80-0417R

Study of Nonadiabatic Boundary-Layer Stabilization Time in a Cryogenic Tunnel for Typical Wing and Fuselage Models

Charles B. Johnson*
NASA Langley Research Center, Hampton, Va.

A theoretical study has been made of the time varying effect of nonadiabatic wall conditions on boundary layer properties for a two-dimensional wing section and an axisymmetric body of revolution typical of a fuselage. The wing section and body of revolution are representative of the root chord and fuselage of what is considered to be a typical size transport model for the National Transonic Facility. The transient analysis was made at a Mach number of 0.85, for stagnation pressures of 2, 6, and 9 atm at several cryogenic values of total temperature for a solid wing and for three different fuselage skin thickness configurations. The analysis considered wing and fuselage sections made from stainless steel, beryllium copper, and aluminum. Examples are presented that may be used to determine the time required to reach an adiabatic condition after a change in total temperature.

Nomenclature

C_D = section drag coefficient, drag/qc
C_f = local skin-friction coefficient, shear stress/q
c = chord of NACA 0012-64 airfoil, cm
$\bar{c}$ = mean geometric chord, cm
C_p = pressure coefficient, $p-p_\infty/q_\infty$
h = heat transfer coefficient, heat transfer rate/$(T_{aw}-T_w)$, W/m^2 K
L = length of NASA bodies of revolution, 121.92 cm
M = Mach number
p = pressure, atm
q = dynamic pressure, atm
R_c = Reynolds number, based on a chord of 25.4 cm
$R_{\bar{c}}$ = Reynolds number, based on $\bar{c}$
T = temperature, K
t = time, s
x = distance along chord of airfoil or centerline of body of revolution, cm
α = angle of attack, deg
δ^* = boundary layer displacement thickness, cm
τ = model skin thickness, cm

Subscripts

aw = adiabatic wall conditions
i = initial conditions
s = surface conditions
t = stagnation conditions
w = wall condition
∞ = freestream conditions

Introduction

THE National Transonic Facility (NTF),[1-3] currently being constructed at the NASA Langley Research Center, is a most technologically advanced wind tunnel. This cryogenic facility provides the capability for testing over a large range of Reynolds numbers (to full scale for most aircraft) while avoiding many of the practical problems associated with achieving high Reynolds numbers in conventional pressure tunnels. The large range of Reynolds numbers in the NTF is obtained by varying the total temperature and total pressure.

From the standpoint of operational flexibility and economy, it is desirable to change the Reynolds number rapidly during a given test by as close to a step change in total temperature as possible. After a rapid change in total temperature, the model will not be in thermal equilibrium with respect to its surroundings, but will, over a period of time, be cooling (or heating) toward its adiabatic wall condition. In order to determine the usability of this rapid, almost step change, in total temperature for aerodynamic testing, an evaluation is being made to determine the time required for the model to reach an adiabatic wall condition, as well as the effect of a nonadiabatic wall on the boundary-layer properties.

This paper will present results from a theoretical analysis of the time varying effects of nonadiabatic wall conditions on boundary-layer properties for two configurations made from three materials: 1) 310S stainless steel, 2) beryllium copper, and 3) 5083 aluminum alloy. One configuration is a solid NACA 0012-64 airfoil with a 25.4-cm chord. The other configuration is a NASA body of revolution, referred to as body 11,[4] with a length of 121.92 cm. The body of revolution was analyzed as a solid body, a body with a 2.54-cm-thick skin and a body with a 1.27-cm-thick skin.

Basis for Analysis

It is well known that one of the major testing advantages of a cryogenic wind tunnel is the expanded testing envelope resulting from the ability to vary total temperature over a wide range. This advantage is illustrated in Fig. 1, which shows a typical testing envelope for the NTF at a test section Mach number of 0.8. The operating envelope is bounded above by a maximum operating pressure of 9 atm based on the structural limit of the pressure shell. The lower bound of minimum pressure is slightly greater than atmospheric pressure to allow for venting so that additional cooling gas can be introduced into the tunnel. The maximum total temperature boundary on the left is about 340 K coupled with restraints dictated by the drive system. The boundary on the right is determined by a minimum total temperature at which condensation is avoided. (This illustration is based on condensation occurring when the local Mach number reaches 1.4, which for $p_t = 6.65$ atm, is at $T_t = 117$ K.) T_t varies over the pressure range from 96 K at the minimum pressure to 122 K at the maximum pressure. The operating characteristics allow the unique capability of pure Reynolds number studies, at a constant pressure, by the appropriate changes in total temperature, as indicated by the horizontal line in Fig. 1. Pure aeroelastic studies at a constant Reynolds number (as in-

Presented as Paper 80-0417 at the AIAA 11th Aerodynamic Testing Conference, Colorado Springs, Colo., March 18-20, 1980; submitted March 18, 1980; revision received April 27, 1981. This paper is declared a work of the U.S. Government and therefore is in the public domain.

*Aerospace Engineer, Subsonic-Transonic Aerodynamics Division. Member AIAA.

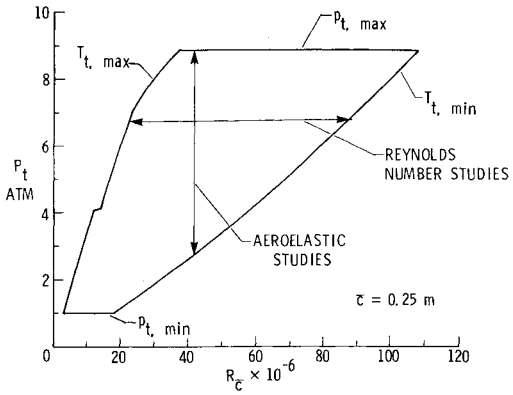

Fig. 1 Total pressure and temperature limits for the NTF operating envelope at $M_\infty = 0.80$.

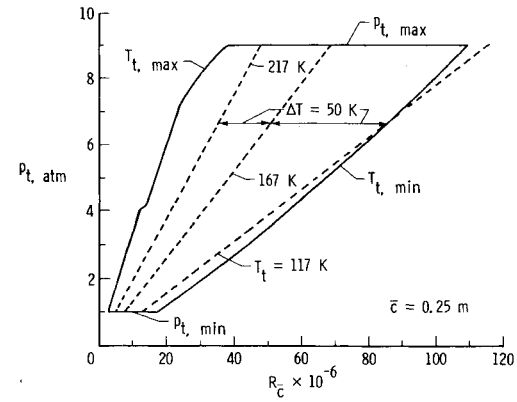

Fig. 2 Total temperature change in a pure Reynolds number study for the NTF operating envelope at $M_\infty = 0.80$.

dicated by the vertical line in Fig. 1) are obtained by varying the total pressure and the appropriate adjustment of the total temperature. The variation of Reynolds number with temperature is nonlinear,[5] with the greatest change in Reynolds number per unit temperature change occurring at the lowest temperature. Therefore the present analysis was made for a ΔT of 50 K between temperatures of 167 and 117 K, which corresponds to a Reynolds number range for the NTF from 50×10^6 to 85×10^6 at 6.65 atm, as indicated in Fig. 2. In this phase of the investigation, a step change in temperature was assumed. This gives a somewhat optimistic estimate of the time required for the model to reach adiabatic conditions. The actual time required to make a 50 K temperature change in the NTF was not known at the time of this analysis, however, it is now estimated to be on the order of 15-30 s at pressures of 2-6 atm.

A rapid decrease in total temperature means that the recovery temperature of the flow will be less than the temperature of the model and that, for a period of time, the model will be cooling toward its adiabatic wall temperature. The consequent heat transfer will significantly affect the boundary layer properties until the adiabatic wall condition is approached. It was noted by Kilgore,[5] that results from boundary-layer calculations in which an ideal-gas method (i.e., flight calculations) was compared to a real-gas cryogenic method of calculation (i.e., NTF application) showed that if both the real-gas and ideal-gas results are at adiabatic wall conditions, there is virtually no difference in boundary-layer properties. Therefore this paper will examine the variation, with time, of the local skin friction and boundary-layer displacement thickness from the time at which total temperature is changed until the time the model reaches an adiabatic wall condition. For all the conduction calculations presented in this paper, it is assumed that a step change in total temperature from 167 to 117 K at $t = 0$ s has been made.

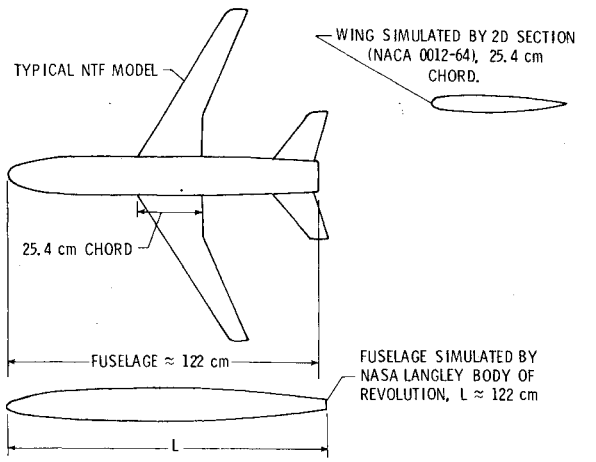

Fig. 3 Simulation of wing and fuselage sections for conduction analysis.

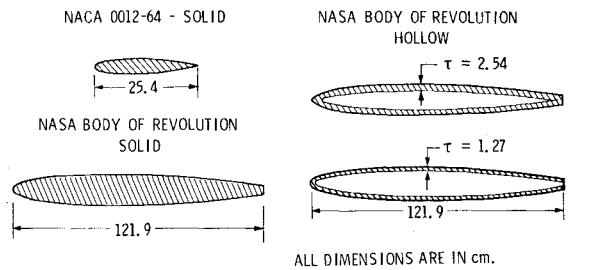

Fig. 4 Four models used in conduction analysis.

Method of Analysis

The geometry used in the conduction analysis for wing and fuselage simulation is shown in Fig. 3 in relation to a model of an airplane sized for use in the National Transonic Facility (NTF). The fuselage is simulated by a NASA body of revolution with a length of about 122 cm and a thickness-to-length ratio of about 0.105. The root section of the wing is simulated by the NACA 0012-64 airfoil section. The geometry of the four configurations that were analyzed is shown in Fig. 4. The NACA 0012-64 airfoil was input into the conduction code as a solid body. Three mass configurations of the NASA body of revolution were used in the conduction analysis, one solid and two hollow. The two hollow configurations had wall thicknesses of 2.54 and 1.27 cm. An outline of the six steps used in the method of analysis follows.

1) Determine heating rates to the NACA 0012-64 airfoil section and NASA body of revolution at $M_\infty \approx 0.85$, $\alpha = 0$ using measured surface pressures.

2) Determine the effect of wall to total temperature ratio (T_w/T_t) and stagnation pressure on heating rates of bodies of revolution.

3) Discretize the two-dimensional airfoil and body of revolution into conduction and storage nodes.

4) Input heat transfer coefficients and nodal geometry into transient heat conduction code and determine temperature history for 310S stainless steel, beryllium copper, and 5083 aluminum alloy, with step changes in total temperature at time equal to zero.

5) Make boundary-layer calculations for various T_w/T_t ratios over a range of values of T_t and p_t for both the NACA 0012-64 airfoil and the NASA body of revolution.

6) Evaluate error, due to nonadiabatic wall conditions, in boundary layer properties relative to adiabatic conditions by combining results of steps 4 and 5.

Subsequent sections of this paper describe in detail each of the preceding steps and results will be presented, in terms of the stabilization times, for skin friction and boundary-layer displacement thickness.

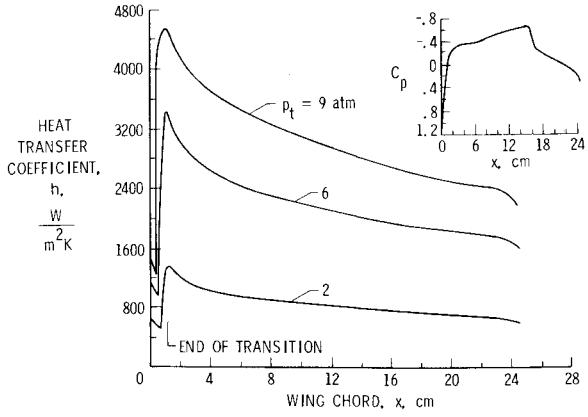

Fig. 5 Effect of pressure on the heat transfer coefficient on the NACA 0012-64 airfoil ($M_\infty = 0.85$, $\alpha = 0$, $T_t = 116$ K, $c = 25.4$ cm, $T_w/T_t = 1.22$).

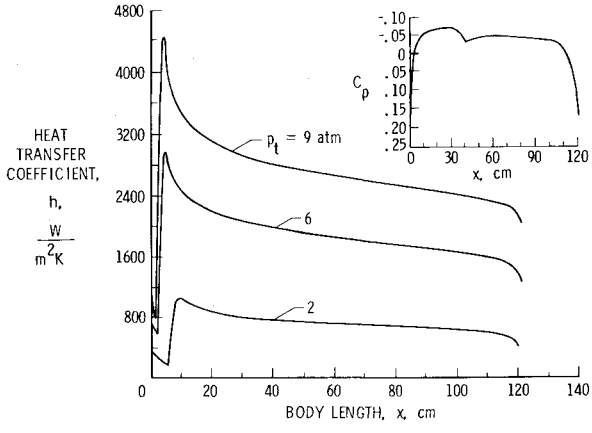

Fig. 6 Effect of pressure on the heat transfer coefficient on the NASA body of revolution ($M_\infty = 0.85$, $\alpha = 0$, $T_t = 116$ K, $L = 121.9$ cm, $T_w/T_t = 1.22$).

Results and Discussion

Heat Transfer Effects

The distribution of the heat transfer coefficient (calculated by the method of Anderson and Lewis[6]) over the NACA 0012-64 airfoil and the NASA body of revolution for stagnation pressures of 2, 6, and 9 atm is shown in Figs. 5 and 6, respectively. The pressure distributions shown on the insert in the figures are fairings of experimental data[4,7] and were used as input to the calculation. At $p_t = 2$ atm, the beginning of transition was assumed to be about 3 and 4% of chord (and length) for the NACA 0012-64 and the NASA body of revolution, respectively. At the higher pressures, the start of transition moves upstream as would be expected. The heat transfer coefficient distribution was calculated at a mean value of $T_w/T_t = 1.22$, which falls midway between the initial value of 1.41 and the final (i.e., adiabatic) value of about 0.985. These calculated heat transfer coefficient distributions were used as an input for the heat conduction analysis which uses a constant value for the heat transfer coefficient distribution; hence the mean value ($T_w/T_t = 1.22$) was used as an approximation to a time-varying value.

The variation of surface temperature at three locations on the NACA 0012-64 airfoil made of stainless steel is shown in Fig. 7. The temperature variations in Fig. 7 and all other transient temperature results were obtained from a transient conduction program.[8] The program obtains a solution for temperatures using the backward finite difference method for the heat balance equations. As can be seen, the trailing edge of the airfoil, which has a relatively small mass, rapidly approaches the adiabatic wall temperature in about 30 s. The

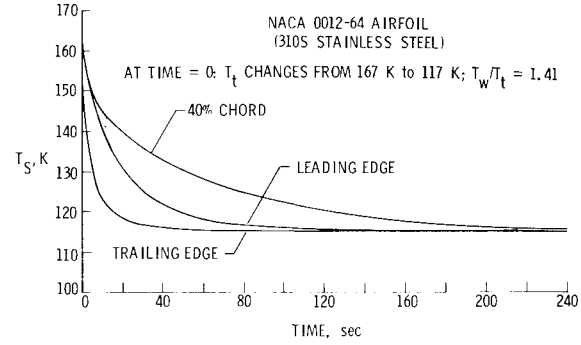

Fig. 7 Variation of surface temperature with time after a 50 K step change ($M_\infty = 0.85$, $p_t = 2$ atm, $T_i = 164.5$ K, $T_{aw} = 115.2$ K, $c = 25.4$ cm).

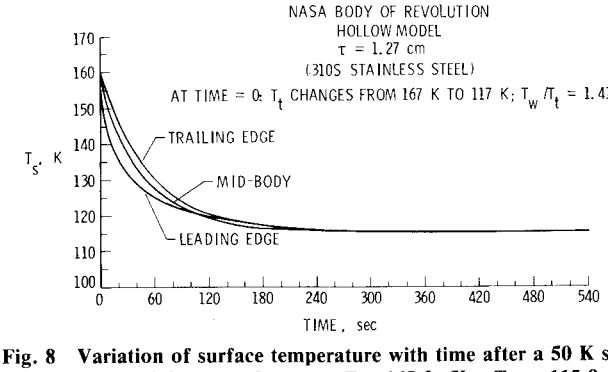

Fig. 8 Variation of surface temperature with time after a 50 K step change ($M_\infty = 0.85$, $p_t = 2$ atm, $T_i = 165.3$ K, $T_{aw} = 115.8$ K, $L = 121.9$ cm).

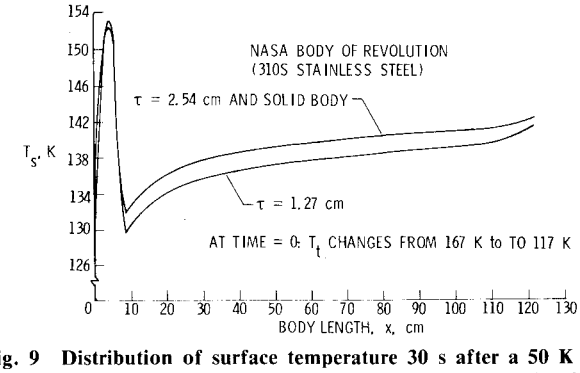

Fig. 9 Distribution of surface temperature 30 s after a 50 K step change ($M_\infty = 0.85$, $p_t = 2$ atm, $T_i = 165.3$ K, $T_{aw} = 115.8$ K, $L = 121.9$ cm).

leading edge approaches the adiabatic temperature more slowly because of the increased mass in the leading edge compared to the trailing edge. In the region of maximum thickness (at the 40% chord), it takes almost 4 min to approach the adiabatic temperature.

The variation of surface temperature with time at three locations on the NASA body of revolution is shown in Fig. 8. The wall thickness for this particular configuration is 1.27 cm and the material is stainless steel. It can be seen from Fig. 4, that this configuration has about the same mass (per unit area) at the leading edge, trailing edge, and midbody, thus the rate at which these locations approach the adiabatic wall value is primarily dependent on the heat transfer coefficient at the respective locations (see Fig. 6). The stagnation point at the nose of the body has the highest heat transfer coefficient ($h = 1301$ W/m^2 K) and thus cools more rapidly. The midbody station cools somewhat slower than the nose, and the trailing edge, which has the lowest heat transfer coefficient, cools the slowest. All three stations reach the adiabatic wall

value at about 240 s after the 50 K step change in total temperature.

The distribution of surface temperature over the three configurations of the NASA body of revolution 30 s after the 50 K step change in total temperature is shown in Fig. 9. The peak temperature at $x \approx 5$ cm corresponds to the beginning of transition which is seen in the heat transfer coefficient distribution in Fig. 6. At this time, after the step change in total temperature, the surface temperature distribution is quite sensitive to the distribution of the heat transfer coefficient over the model. In particular, the location of the beginning and end of transition will strongly affect the temperature distribution over the model.

Aerodynamic Effects

The results from Figs. 7-9 and additional calculations indicated that the time required to reach an adiabatic condition over the entire model might be quite long particularly for a solid body of revolution. In an effort to determine a nonadiabatic level (i.e., a T_w/T_t ratio) that would be acceptable for testing, calculations of the section drag coefficient of the NACA 0012-64 airfoil as a function of T_w/T_t were made (see Fig. 10) at $R_c = 27.1 \times 10^6$ ($p_t = 2$ atm). Initially, an adiabatic ($T_w/T_t \approx 0.985$) method of calculation was used to determine the adiabatic value of C_D. This adiabatic drag coefficient was determined from the two-dimensional airfoil code of Bauer et al.[9] The nonadiabatic ($0.4 < T_w/T_t < 2.5$) and adiabatic values of skin friction drag for the NACA 0012-64 airfoil were calculated from the Anderson-Lewis[6] code. These boundary layer calculations were all made using the same pressure distribution over the airfoil and a beginning of transition fixed between 2 and 5% of the chord for all T_w/T_t ratios. The variation of section drag coefficient with T_w/T_t shown in Fig. 10, was obtained by subtracting the adiabatic value of skin friction drag out and adding in the nonadiabatic values at various T_w/T_t ratios. It can be seen in Fig. 10 that, plus or minus, one drag count on either side of the adiabatic value of C_D ($T_w/T_t = 0.985$) corresponds to T_w/T_t ratios of 0.90 and 1.08. Thus, when a model that is being cooled reaches a T_w/T_t ratio of 1.08, the nonadiabatic effects cause the drag to be one drag count less than the adiabatic value of drag. Based on this analysis (Fig. 10), it appears that for a model that is being cooled, data could be taken when the model reaches a T_w/T_t ratio of 1.08.

As was previously noted, the variation in drag in Fig. 10 is due only to the variation in friction drag with a change of T_w/T_t ratio for a fixed pressure distribution and a nearly constant location of transition. Figure 10 shows an increase in drag with a decreasing T_w/T_t ratio. However, as the wall is cooled, the slope of the curve in Fig. 10 may actually change direction if both the boundary layer stability[10] (i.e., increase in transition Reynolds number) and the pressure distribution (i.e., shock location and wake separation characteristics) are significantly affected by wall cooling. Thus, in an actual wind tunnel test, the total drag on a 2-D airfoil may decrease as the T_w/T_t ratio is decreased. This change in the drag curve with

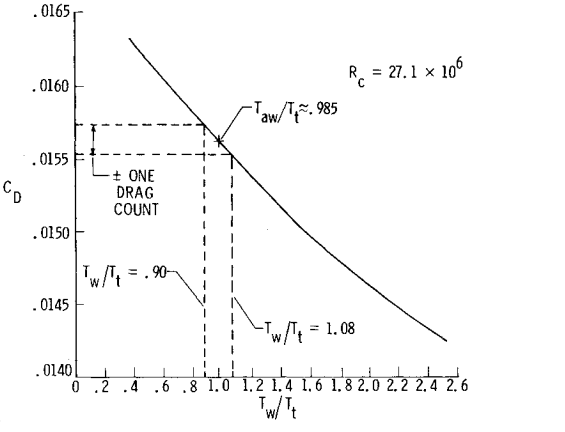

Fig. 10 Section drag coefficient of the NACA 0012-64 airfoil as a function of T_w/T_t ratio ($M_\infty = 0.85$, $p_t = 2$ atm, $T_t = 116$ K, $c = 2.54$ cm).

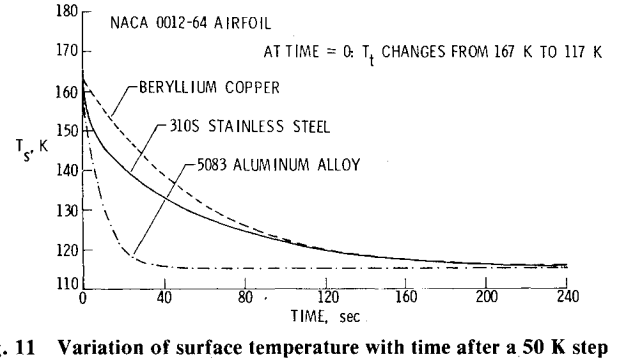

Fig. 11 Variation of surface temperature with time after a 50 K step change for different metals ($M_\infty = 0.85$, $p_t = 2$ atm, $x/c = 0.4$, $c = 25.4$ cm).

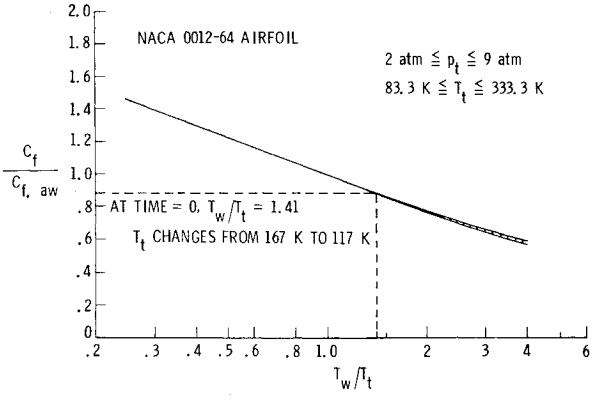

Fig. 12 Variation of the local skin friction ratio with T_w/T_t ratio over a range of stagnation conditions ($M_\infty = 0.85$, $x/c = 0.4$, $c = 25.4$ cm).

Table 1 Comparison of cool down times (s) for two materials to reach a $T_w/T_t = 1.08$ after a 50 K step change

	310S stainless steel			Beryllium copper		
Configuration, atm	$p_t = 2$	$p_t = 6$	$p_t = 9$	$p_t = 2$	$p_t = 6$	$p_t = 9$
NACA 0012-64 ($x/c = 0.4$)	70	24	15	79	34	25
Body of revolution (solid, $x/L = 0.5$)	142	32	18	234	92	65
Body of revolution ($r = 2.54$ cm, $x/L = 0.5$)	115	31	18	154	61	42
Body of revolution ($r = 1.27$ cm, $x/L = 0.5$)	65	25	16	83	33	24

T_w/T_t would undoubtedly change the values of the T_w/T_t ratios for an error of one drag count that were established in Fig. 10.

A comparison of the cool down times for 310S stainless steel and beryllium copper to reach a value of $T_w/T_t = 1.08$ are shown in Table 1 for a Mach number of 0.85 and stagnation pressures of 2, 6, and 9 atm. The cool down follows a step change in total temperature from 167 to 117 K at time equal to zero. At all the stagnation pressures for the four configurations, the stainless-steel models reach the $T_w/T_t = 1.08$ ratio in a shorter period of time than the beryllium copper models. For the airfoil, the times for the two materials are within 10 s of each other; however, for the solid body of revolution, the time difference to reach a ratio of 1.08 is much longer for the beryllium copper than for the 310S stainless steel. For instance, at pressure of 2 atm, the beryllium copper takes 92 s longer than the stainless steel to reach $T_w/T_t = 1.08$. At a pressure of 9 atm, the solid body of revolution made from beryllium copper takes about 3.6 times longer to reach the $T_w/T_t = 1.08$ ratio than the stainless-steel configuration.

A comparison of the surface temperature vs time on the NACA 0012-64 airfoil ($x/c = 0.4$) for three different materials is shown in Fig. 11. These time histories show that the 5083 aluminum alloy airfoil reaches an adiabatic wall temperature in about 50 s compared to the 4 min required for the beryllium copper airfoils and 310S stainless steel. It is interesting to note that, for the first 2 min of cooling, the 310S stainless-steel airfoil approaches the adiabatic wall temperature more rapidly than the beryllium copper airfoil. However, after about 2 min, the stainless steel and beryllium copper airfoils have about the same temperature-time history.

In addition to the foregoing brief analysis of drag presented in Fig. 10, the variations of skin friction coefficient and boundary-layer displacement thickness with T_w/T_t were investigated over the total range of tunnel operation temperature and pressure. The variation in the ratio of the local skin friction relative to the adiabatic wall value at $x/c = 0.4$ ($M_\infty = 0.85$) on the NACA 0012-64 airfoil is shown in Fig. 12 as a function of the wall-to-total temperature ratio. The variation of the $C_f/C_{f,aw}$ ratio in Fig. 12 was calculated using the boundary layer code of Harris[11] over a range of stagnation pressures from 2 to 9 atm and a range of stagnation temperatures from 83.3 to 333.3 K. As shown in Fig. 12, when the local skin friction is ratioed to the adiabatic wall values of C_f, the resulting $C_f/C_{f,aw}$ ratio (for the range of stagnation conditions shown) collapses to a single curve independent of both stagnation pressure and stagnation temperature. A similar curve to that of Fig. 12 was developed for the ratio of local boundary layer displacement thickness relative to the adiabatic wall value at $x/c = 0.4$ on the NACA 0012-64 airfoil. The δ^*/δ^*_{aw} ratio as a function of T_w/T_t is also independent of stagnation temperature from 83.3 to 333.3 K. However, the δ^*/δ^*_{aw} ratio is slightly dependent on stagnation pressures, and individual curves for stagnation pressures of 2, 6, and 9 atm were used in the analysis of heat conduction. For all such analyses presented in this paper, the initial temperature condition (at time = 0) corresponds to a wall-to-total temperature ratio of 1.41 (at time = 0, T_t changes from 167 to 117 K). At this condition, indicated by the dashed line in Fig. 12, the local skin friction is about 88% of the adiabatic wall value. Similar calculations of $C_f/C_{f,aw}$ and δ^*/δ^*_{aw} were made for the NASA body of revolution at stagnation pressures of 2, 6, and 9 atm and stagnation temperatures from 83.3 to 333.3 K. The dependency on the stagnation pressure and temperature of the C_f and δ^* ratios for the body of revolution was about the same as that for the airfoil.

Boundary-Layer Stabilization Time

The boundary-layer stabilization time due to nonadiabatic wall conditions as a function of time are determined by combining the results from the transient heat conduction code, such as shown in Figs. 7 and 8, with the boundary-layer analysis of $C_f/C_{f,aw}$ and δ^*/δ^*_{aw} shown typically in Fig. 12. The results of combining a boundary-layer analysis with the heat conduction results for the NACA 0012-64 airfoil made from 310S stainless steel are shown in Figs. 13 and 14, at $x/c = 0.4$. Similar results for the NASA body of revolution at $x/L = 0.5$ are shown in Figs. 15 and 16 for the solid body and Figs. 17 and 18 for the body with $\tau = 1.27$ cm. The results for the body of revolution with $\tau = 2.54$ cm are given in Ref. 12 and in Table 2. Table 2 summarizes the stabilization times for the four configurations at $M_\infty = 0.85$, for stagnation pressures of 2, 6, and 9 atm. Included in the table are the maximum error (at time = 0), the time to reduce the maximum error by 50%, the time to reach a $T_w/T_t = 1.08$ ratio (based on analysis from Fig. 10), and the time to reach an adiabatic condition. The times required for the four configurations to reduce the maximum error by 50% are considerably less than the times required to reach an adiabatic condition as can be seen from Table 2. The pronounced increase in the time to reach an adiabatic condition over the time to reduce the maximum error by 50% is due to the nonlinearity of the curves in Figs. 13-18. It should be remembered that the analysis is based on the model being at an initial uniform equilibrium temperature of about 164.5 K and then at time = 0 there is a step change in total temperature from 167 to 117 K.

The solid NACA 0012-64 airfoil (Figs. 13 and 14) requires about 300 s to reach an adiabatic condition at a stagnation pressure of 2 atm and 200 and 180 s at stagnation pressures of 6 and 9 atm, respectively. The time for the airfoil to reach $T_w/T_t = 1.08$ is about 70 s for the 2-atm condition and somewhat less for the 6- and 9-atm conditions. The errors at the $T_w/T_t = 1.08$ condition are about 3 and 6% for the C_f and

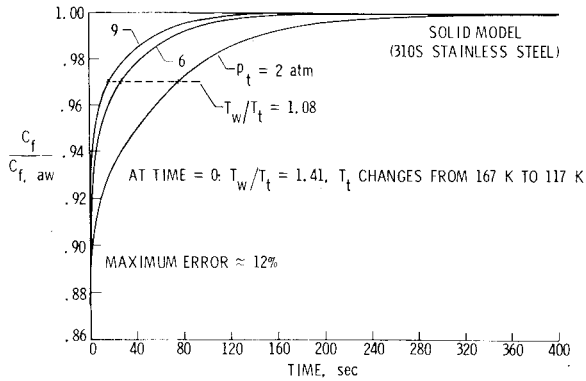

Fig. 13 Departure of the local skin friction from the adiabatic wall value as a function of time for the NACA 0012-64 airfoil ($M_\infty = 0.85$, $x/c = 0.4$, $c = 25.4$ cm).

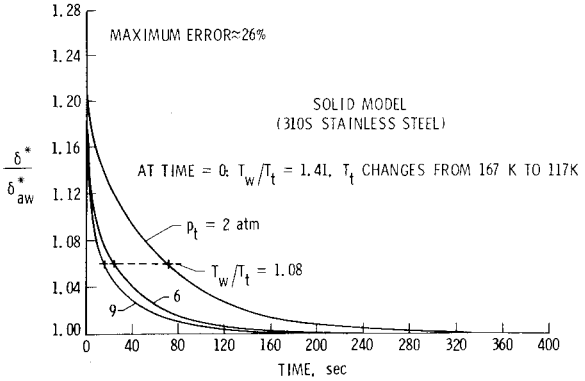

Fig. 14 Departure of displacement thickness from the adiabatic wall value as a function of time for the NACA 0012-64 airfoil ($M_\infty = 0.85$, $x/c = 0.4$, $c = 25.4$ cm).

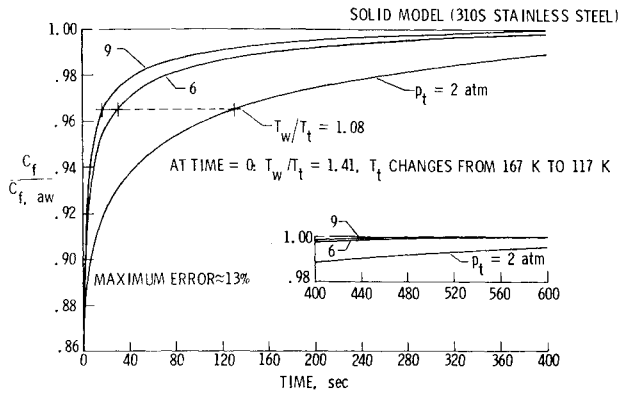

Fig. 15 Departure of local skin friction from the adiabatic wall value as a function of time for the NASA body of revolution ($M_\infty = 0.85$, $x/L = 0.5$, $L = 121.92$ cm).

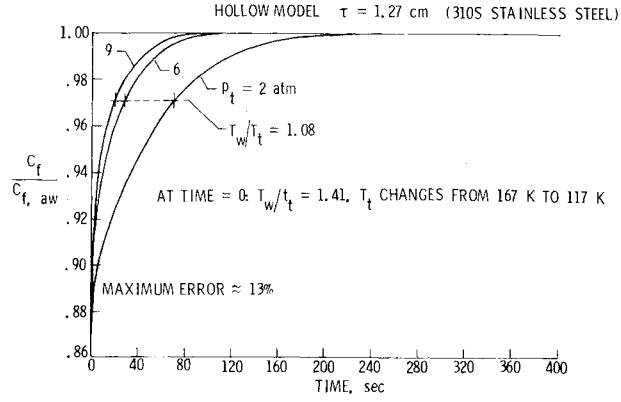

Fig. 17 Departure of local skin friction from the adiabatic wall value as a function of time for the NASA body of revolution ($M_\infty = 0.85$, $x/L = 0.5$, $L = 121.92$ cm).

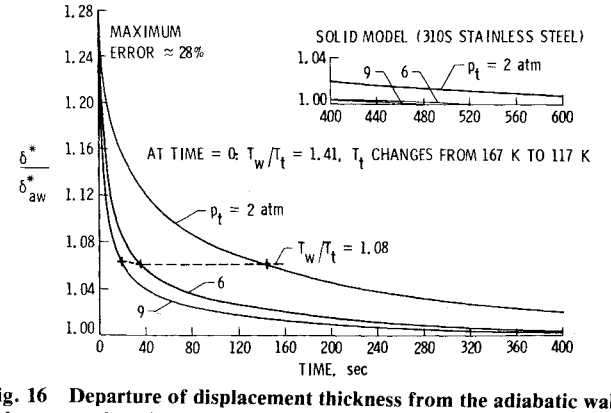

Fig. 16 Departure of displacement thickness from the adiabatic wall value as a function of time for the NASA body of revolution ($M_\infty = 0.85$, $x/L = 0.5$, $L = 121.92$ cm).

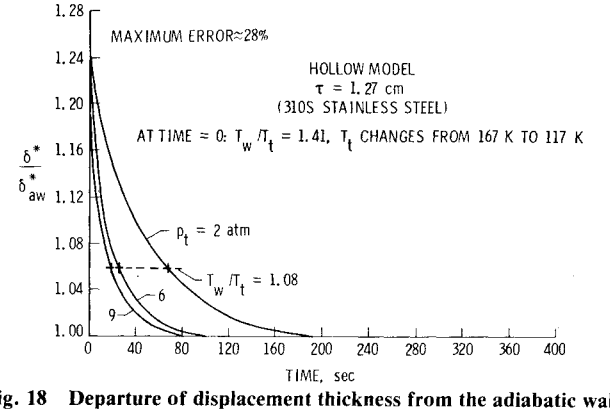

Fig. 18 Departure of displacement thickness from the adiabatic wall value as a function of time for the NASA body of revolution ($M_\infty = 0.85$, $x/L = 0.5$, $L = 121.92$ cm).

Table 2 Boundary layer stabilization times for four configurations after a 50 K step change (310S stainless steel)

		$p_t = 2$ atm			$p_t = 6$ atm			$p_t = 9$ atm		
	Approx. max. error, %	Time max. error reduced by 50%, s	Time to reach $T_w/T_t = 1.08$, s	Time to reach adiabatic condition, s	Time max. error reduced by 50%, s	Time to reach $T_w/T_t = 1.08$, s	Time to reach adiabatic condition, s	Time max. error reduced by 50%, s	Time to reach $T_w/T_t = 1.08$, s	Time to reach adiabatic condition, s
					$C_f/C_{f,aw}$					
NACA 0012-64 ($x/c = 0.4$)	12	28	70	300	6	24	200	3	15	180
Body of revolution (solid, $x/L = 0.5$)	13	37	142	>600	9	32	540	6	18	480
Body of revolution ($\tau = 2.54$ cm, $x/L = 0.5$)	13	36	115	390	9	31	235	5	18	205
Body of revolution ($\tau = 1.27$ cm, $x/L = 0.5$)	13	29	65	200	8	25	100	5	16	85
					δ^*/δ^*_{aw}					
NACA 0012-64 ($x/c = 0.4$)	26	21	70	300	4	24	200	2	15	180
Body of revolution (solid, $x/L = 0.5$)	28	29	142	>600	8	32	540	4	18	480
Body of revolution ($\tau = 2.54$ cm, $x/L = 0.5$)	28	29	115	390	8	31	235	4	18	205
Body of revolution ($\tau = 1.27$ cm, $x/L = 0.5$)	28	25	65	200	7	25	100	4	16	85

δ^* analyses, respectively, for all pressures as can be seen in Figs. 13 and 14 (as expected from the results of Fig. 12).

The times to reach an adiabatic condition for the NASA body of revolution from the 2-atm condition, range from a time slightly greater than 600 s for the solid body to 390 and 200 s for the $\tau = 2.54$- and 1.27-cm hollow bodies, respectively (see Table 2). The solid body of revolution reaches an adiabatic condition in about 540 and 480 s for the 6- and 9-atm condition, respectively. The thicker walled hollow body of revolution[12] ($\tau = 2.54$ cm) reaches an adiabatic condition in about 210 s for the 6- and 9-atm condition. The thinner walled hollow body of revolution ($\tau = 1.27$ cm) reaches an adiabatic condition in 100 and 85 s for the 6- and 9-atm condition, respectively. The times to reach the $T_w/T_t = 1.08$ condition for the 2-atm stagnation pressure are 142, 115, and 65 s for the solid, $\tau = 2.54$- and 1.27-cm hollow bodies of revolution, respectively. At the two higher pressures, the times to reach $T_w/T_t = 1.08$ are significantly reduced as can be seen in Table 2. For the C_f and δ^* analyses, the errors at the $T_w/T_t = 1.08$ condition are about 3 and 6% at all pressures, for all three configurations of the body of revolution.

Concluding Remarks

A theoretical analysis of the time varying effects of nonadiabatic wall conditions on boundary-layer properties has been made for representative elements of a typical model for the National Transonic Facility cryogenic wind tunnel. The elements analyzed were 1) a solid airfoil section representative of the root-section of a subsonic transport model and 2) an axisymmetric body with varying degrees of skin thickness representative of the fuselage. The results of the analysis showed that when the wall temperature of the airfoil was 1.08 times the total temperature of the test medium, the error in drag coefficient was only one count. These results provide a convenient basis for evaluating the time varying effects which were calculated for the case of a 50 K instantaneous drop in temperature from 167 to 117 K. The results of the time varying analysis show that if the body is made hollow with a moderately thin skin, its time constants are consistent with those of the airfoil and that the time required to accommodate the temperature change is not excessive. For example, the time required for both parts of a model to reach a temperature of no more than 1.08 times the test medium total temperature, after the 50 K reduction in gas temperature, is about 70 s for tests at a total pressure of 2 atm and only about 15 s at a pressure of 9 atm.

References

[1] Nicks, O.W. and McKinney, L.W., "Status and Operational Characteristics of the National Transonic Facility," paper presented at the AIAA 10th Aerodynamic Testing Conference, San Diego, Calif., April 1978.

[2] McKinney, L.W. and Howell, R.R., "The Characteristics of the Planned National Transonic Facility," paper presented at the AIAA 9th Aerodynamic Testing Conference, Arlington, Texas, June 1976.

[3] Howell, R.R. and McKinney, L.W., "The U.S. 2.5 Meter Cryogenic High Reynolds Number Tunnel," paper presented at the 10th Congress of the International Council of the Aeronautical Sciences (ICAS), Ottawa, Canada, Oct. 1976.

[4] Chudyk, D.W., "Transonic Wind Tunnel Tests of Several NASA Bodies of Revolution," NASA CR 112069, 1971.

[5] Kilgore, R.A., Igoe, W.B., Adcock, J.B., Hall, R.M., and Johnson, C.B., "Full Scale Aircraft Simulation With Cryogenic Tunnels and Status of the National Transonic Facility," paper presented at the International Symposium on Cryogenic Wind Tunnels, Southampton, England, April 1979.

[6] Anderson, E.C. and Lewis, C.H., "Laminar or Turbulent Boundary-Layer Flows of Perfect Gases of Reacting Gas Mixtures in Chemical Equilibrium," NASA CR 1893, Oct. 1971.

[7] Hall, R.M., "An Analysis of Data Related to the Minimum Temperatures for Valid Testing in Cryogenic Wind Tunnels Using Nitrogen as the Test Gas," NASA TM X-73924, Aug. 1976.

[8] Haas, L.A., "A Study of a Fail-Safe Abort System for an Actively Cooled Hypersonic Aircraft," NASA CR 144927, Dec. 1975.

[9] Bauer, F., Garabedian, P., and Korn, D. *Supercritical Wing Sections III, Lecture Notes in Economics and Mathematical Systems,* Vol. 150, Springer-Verlag, New York, 1977.

[10] Reshotko, E. "Drag Reduction by Cooling in Hydrogen Fueled Aircraft," *Journal of Aircraft,* Vol. 16, Sept. 1979, p. 584-590.

[11] Harris, J.E., "Numerical Solution of the Equations for Compressible Laminar, Transitional and Turbulent Boundary-Layers and Comparisons with Experimental Data," NASA TR R-368, Aug. 1971.

[12] Johnson, C.B., "Theoretical Study of Nonadiabatic Boundary-Layer Stabilization Times in a Cryogenic Wind Tunnel for Typical Stainless-Steel Wing and Fuselage Models," NASA TM 80212, July 1980.